COMMUNICATIONS IN SCIENCE AND TECHNOLOGY
Homepage: cst.kipmi.or.id

Composite copper(I)-hydroxyapatite: a heterogeneous catalyst for the homocoupling reaction of biaryl compounds

Iis Intan Widiyowati[a,b], *Atiek Rostika Noviyanti*[a,*], Mukhamad Nurhadi[b], Muhamad R. S. Sidik[a], Muhammad R. Ramadhan[a], Yudha Prawira Budiman[a]

[a]*Department of Chemistry, Universitas Padjadjaran, Sumedang 45363, Indonesia*
[b]*Department of Chemical Education, Universitas Mulawarman, Samarinda, 75119, Indonesia*

Article history:
Received: 14 May 2026 / Received in revised form: 21 June 2026 / Accepted: 22 June 2026

Abstract

In this present study, a reusable Cu(I)-hydroxyapatite (HAp) catalyst was developed for the homocoupling of arylboronic acids under mild conditions. The investigation encompassed the examination of how different solvents and atmospheric conditions affect the performance of catalyst. The catalyst, was prepared by means of wet impregnation with an acetone-water (24:1) mixture purposely to load 10 wt% CuI onto HAp. XRD, FT-IR, and SEM-EDS analyses demonstrated that CuI was successfully deposited on the HAp surface without changing its crystal structure or shape. During the experiment, it is established that both the solvent and the atmosphere exhibited a significant impact on the homocoupling of p-tolylboronic acid. The most optimal results were achieved through the utilization of dry DMF in air at room temperature for a duration of 24 hours. In these conditions, 4,4'-dimethylbiphenyl was isolated in approximately 80% yield, as confirmed by GC-MS, ^{1}H NMR, and ^{13}C NMR. The catalyst stayed active over four cycles, although the yield fell to 53% by the fourth run. XRD analysis of the used catalyst revealed that the HAp structure remained mostly unchanged. When we tested different substrates, it was found that Cu(I)-HAp worked most effectively with para-substituted arylboronic acids that were less densely populated. Overall, Cu(I)-HAp has been identified to a potentially effective heterogeneous catalyst for the aerobic biaryl synthesis. The device is characterized by Its ease of use, its capacity for recycling, and its operationalization at room temperature.

Keyword: Organoboron; biaryl; catalysis; copper; homocoupling

1. Introduction

Biaryl motifs are important building blocks in modern organic chemistry in view of their occurrence in many valuable compounds, including natural products, pharmaceuticals, catalysts, agrochemicals, and materials. For example, this structure has been identified in natural products such as gossypol [1,2] and michellamine B [3,4], as well as in bioactive compounds including magnolol [5–8] and honokiol [7–10] (Fig. 1), which exhibit to possess a range of biological activities. In the field of medicine, biaryl frameworks are part of significant drugs including losartan and valsartan [11–13]. They also play a major role in asymmetric catalysis, where biaryl units are essential in chiral BINAP-type ligands [14,15] and BINOL-based organocatalysts [16,17]. Beyond the realm of medicine and catalysis, biaryl compounds are substantial in the domain of materials science, as seen in 5CB, a common liquid-crystal component [18–21], and CBP, a popular host material in OLED devices [22–24]. In agriculture, this motif has been observed in fungicides such as boscalid [25,26]. The widespread presence and diverse functions of these compounds demonstrate that the biaryl motif is not merely a simple aromatic group; rather it is a key molecular structure that can influence biological activity, catalytic performance, and material properties. Consequently. There is a necessity to identify efficient, selective, and sustainable methods for the synthesis of biaryls.

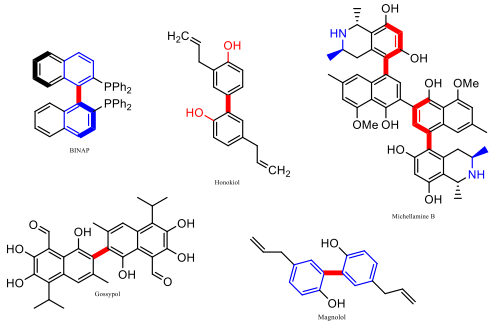

Fig. 1. Representative biaryl-containing compounds

* Corresponding author.
Email: atiek.noviyanti@unpad.ac.id
https://doi.org/10.21924/cst.11.1.2026.1995

Biaryl motifs are of importance in many functional compounds, and the development of direct, efficient, and simple methods for the synthesis of symmetrical biaryls remains a key objective in organic synthesis. In the majority of cases, biaryl frameworks are formed by cross-coupling two distinct prefunctionalised aryl fragments, which are typically an electrophile and a nucleophile. The Suzuki–Miyaura transformation is particularly well recognized for its ability to form aryl–aryl C(sp^2)–C(sp^2) bonds [27–30]. However, for the synthesis of symmetrical biaryls, the homocoupling of arylboronic acids represents a more direct and efficient strategy, since a single type of aryl precursor forms a uniform aromatic dimer. This approach with boron-based reactants is particularly attractive because arylboronic acids are relatively stable and easy-to-handle organoboron reagents that are well suited for carbon–carbon bond-forming reactions [30–32].

Historically, homocoupling approaches can be traced back to the Ullmann reaction, despite the general requirement of classical protocols for high temperatures and stoichiometric quantities of copper. This then leads subsequent developments towards a milder and practical catalytic systems [29,33]. Methodological advances in this field then progressed rapidly, ranging from early $Ag_2O/CrCl_2$-based protocols enabling homocoupling of boronic acids under relatively mild conditions, to copper-based systems operable at room temperature and under open-air conditions, either assisted by 1,10-phenanthroline ligands or employing simple copper salts such as CuCl [34–36]. Recently, there has been an increased focus among researchers on heterogeneous catalyst platforms that are characterized by enhanced ease to separate and reuse. Examples of this include Cu(I)-USY zeolite for homocoupling arylboronic acids, HKUST-1 catalysts for arylboronic acid homocoupling, and Pd-HAp systems for the homocoupling of *p*-tolylboronic acid [12,31,37]. These advances reflect that support is now viewed as an active part of the process, capable of determining catalytic activity, selectivity, and sustainability. Nevertheless, the existing literature reveals several limitations. Firstly, some systems remain dependent on specific ligands. Secondly some systems are relatively complex regarding their supports, and thirdly, some systems are sensitive to substrate electronic properties. In the HKUST-1 system, for example, electron-donating arylboronic acids were reported to be prone to competing hydroxylation products when the reaction was conducted in air [12,37]. Consequently, the focus has shifted to the selection of active phases and support materials that can collectively enhance catalytic efficiency, stability, and ease of catalyst recovery in the homocoupling of arylboronic acids.

In this regard, Cu(I)-HAp composites represent an attractive system as they combine the reactivity of Cu(I) species with the surface characteristics of HAp as a catalytic support. From the standpoint of the active phase, copper-catalysed homocoupling of arylboronic acids is known to involve transmetalation of the aryl group from boron to copper, accompanied by changes in the oxidation state of copper that generate reactive organocopper species. Accordingly, the employment of a Cu(I) precursor such as CuI is relevant as it provides a suitable initial oxidation state for participation in the catalytic cycle while maintaining economic and accessible characteristics [38]. The practical relevance of Cu(I) has also been demonstrated in CuI-USY zeolite systems, which catalysed homocoupling of arylboronic acids under simple conditions, without additives, with good functional-group tolerance, and with catalyst recyclability [12].

From the support perspective, HAp is attractive because it can function both as a catalyst and as a support for dispersing active phases such as nanoparticles or metal cations. Furthermore, HAp can be synthesised with adequate surface area and porosity, possesses good thermal stability, and shows affinity towards organic compounds, making it advantageous for liquid-phase catalysis [39,40]. Moreover, the HAp surface is not inert, as evidenced by spectroscopic studies that revealed the presence of basic OH^- groups, acidic POH sites, and acid–base pairs that contribute to its catalytic properties. These characteristics have been assumed to influence substrate adsorption, boronic acid activation, and stabilisation of active Cu species on the surface [41]. The utilization of HAp in copper-based catalysts has also been reported, including in Cu-exchanged HAp for three-component coupling and HAp-supported Cu(I) for Sonogashira reactions. These studies collectively demonstrate the capacity of HAp to support and maintain the reactivity of Cu centres in C–C bond-forming transformations [42,43]. On this basis, the combination of CuI and HAp may be regarded as a rational system for development as a heterogeneous catalyst for the homocoupling of *p*-tolylboronic acid. This is due to the fact that it has the potential to combine the catalytic activity of Cu(I) with the advantages of HAp as an inexpensive, stable support rich in acid–base sites and readily separable.

Beyond the rationale for combining Cu(I) and HAp, the development of Cu(I)-HAp is also motivated by several advantages relative to previously reported heterogeneous catalytic systems. In comparison with Cu(I)-USY zeolite, HAp provides a less diffusion-restricted surface environment because catalytic sites are not confined within a predominantly microporous framework, which has the potential to improve the accessibility of reactants to active Cu species. In comparison to HKUST-1, HAp is less complicated to prepare, does not require the use of organic linkers, and is commonly more stable in water and humid environments. These factors are important for making durable and practical catalysts. However, while Pd-HAp catalysts are effective in the synthesis of biaryls, their reliance on palladium results in increased costs and reduced economic sustainability. Replacement of Pd with Cu(I) therefore represents an attractive strategy for reducing material costs while maintaining the advantages of heterogeneous catalysis. Consequently, the motivation for developing Cu(I)-HAp extends beyond the preparation of a new composite material and aims to establish a catalytic system that combines catalytic activity, structural stability, economic viability, ease of preparation, catalyst recyclability, and environmental sustainability within a single platform.

Despite the existence of various systems reported for the homocoupling of arylboronic acids, both in the form of homogeneous copper-based catalysts and heterogeneous catalysts such as Cu(I)-USY zeolite, HKUST-1, and Pd-HAp, studies specifically combining Cu(I) as the active phase with HAp as the support for this transformation appear to be limited in scope. A review of the currently available literature reveals that research attention has largely focused on the development of alternative heterogeneous catalysts and the optimisation of reaction conditions. In contrast, exploration of Cu(I)-HAp composites for arylboronic acid homocoupling, particularly

using *p*-tolylboronic acid as substrate has received relatively little attention [12,31,37]. Moreover, the findings of these studies indicate that the performance of heterogeneous catalysts in this reaction is significantly determined by support type, operating conditions, and substrate electronic properties. In the HKUST-1 system, for example, electron-donating substrates have been observed to undergo competing hydroxylation when reactions are performed in air [37]. In contrast, recent mechanistic studies have reaffirmed the significance of transmetalation steps and copper redox behaviour in determining the efficiency of boronic acid homocoupling, such that selection of Cu(I) as the active phase remains relevant for the design of suitable heterogeneous systems [38].

The novelty of the present study therefore does not solely reside in the preparation of a Cu(I)-HAp composite, but rather in the exploration of a heterogeneous catalytic system designed to integrate the advantages of an earth-abundant copper as a catalyst with a chemically stable, low-cost, and environmentally benign HAp support. In contrast to previously reported Cu(I)-USY zeolite, HKUST-1, and Pd-HAp catalysts, the present system seeks to provide a more practical balance between catalytic performance, catalyst stability, economic feasibility, ease of preparation, and catalyst recovery. Furthermore, this present study aims to establish correlations between the physicochemical characteristics of Cu(I)-HAp and its catalytic behavior in the homocoupling of p-tolylboronic acid. Consequently, this work provides two significant contributions. Firstly, it provides a new catalytic material and secondly it offers a better understanding of how support properties and copper speciation influence the performance of heterogeneous catalysts for biaryl synthesis. To further assess the significance of the proposed catalyst relative to the current state of the art, a comparative evaluation against representative homogeneous and heterogeneous catalytic systems reported in the literature is also presented and discussed. The aim of this study is to synthesize and characterize Cu(I)-HAp catalysts, to examine their activity in the homocoupling reaction of p-tolylboronic acid, and to assess their potential as copper-based heterogeneous catalysts that are more economical, stable, and readily recoverable for the synthesis of symmetrical biaryls.

2. Materials and Methods

2.1. Materials

The following substances were employed in the experiment: diammonium hydrogen phosphate (Supelco, ACS Grade), copper iodide (Sigma-Aldrich, 99.99%), 4-methylphenylboronic acid (Sigma-Aldrich, 97%), 3-methylphenylboronic acid (Sigma-Aldrich, 97%), 2-methylphenylboronic acid (Sigma-Aldrich, 95%), 4-biphenylboronic acid (Sigma-Aldrich, 95%), 4-bromophenylboronic acid (Sigma-Aldrich, 95%), 4-fluorophenylboronic acid (Sigma-Aldrich, 95%), 2-methoxyphenylboronic acid (Sigma-Aldrich, 95%), 4-methoxyphenylboronic acid (Sigma-Aldrich, 95%), 4-*tert*-butylphenylboronic acid (Sigma-Aldrich, 95%), *trans*-2-phenylvinylboronic acid (Sigma-Aldrich, 97%), dichloromethane (Supelco, ACS Grade), *N,N*-dimethylformamide (Sigma-Aldrich, anhydrous, 99.8%), *N,N*-dimethylformamide (Supelco, ACS Grade), ethanol (Supelco, ACS Grade), ethyl acetate (Supelco, ACS Grade), n-hexane (Supelco, ACS Grade), and acetonitrile (Supelco, 98%).

2.2. Preparation of HAp and Cu(I)-HAp catalyst

Hydroxyapatite (HAp) powder ($Ca_{10}(PO_4)_6(OH)_2$) was synthesized from calcium sourced from eggshells, employing a method based on a previous study [44]. The calcium source used in this study was eggshells that had been cleaned and calcined. These were then reacted with diammonium hydrogen phosphate under controlled conditions to produce HAp. The product was then filtered, washed, and dried.

The 10 wt% Cu(I)-HAp catalyst was prepared using a reported method, with modifications to the mixing and drying steps for the objectives of this study [45]. HAp (1.0 g) was mixed in an acetone–water solution (25 mL, 24:1 v/v). Subsequently, CuI (0.30 g) was added to achieve a 10 wt% Cu content. The mixture was stirred at room temperature for 48 hours, then filtered and washed with acetone to remove any unbound material. The solid was then subjected to a drying process at temperature of 100 °C for 12 hours purposely to obtain the Cu(I)-HAp catalyst.

2.3. Instrumentation and characterization

The structural and morphological properties of HAp and the Cu(I)-HAp catalyst were characterized using X-ray diffraction (XRD), Fourier transform infrared spectroscopy (FT-IR), scanning electron microscopy (SEM), and particle size analysis (PSA). The XRD patterns were recorded using a Bruker D8 Advance diffractometer to identify the crystalline phases and structural features of the materials. FT-IR spectra were obtained using a PerkinElmer Spectrum 100 spectrometer to examine functional groups and potential interactions between copper species and the HAp matrix. Surface morphology was observed by means of a Hitachi SU3500 scanning electron microscope, while the particle size distribution was analyzed using a Horiba SZ-100.

The biaryl products were characterized by proton nuclear magnetic resonance (^{1}H NMR and ^{13}C NMR) spectroscopy and gas chromatography–mass spectrometry (GC–MS). NMR spectra were recorded on a benchtop 90 MHz NMR spectrometer (Spinsolve 90, Magritek). Chemical shifts (δ) are reported in ppm relative to tetramethylsilane (TMS) as an internal standard, with referencing based on the residual proton signal of the deuterated solvent (CDCl3: 7.26 ppm). GC–MS analyses were performed using an Agilent 7890A gas chromatograph equipped with an Agilent 5977B GC/MSD operating in electron ionization (EI) mode. The separation process was conducted on a DB-5MS column (5% phenylmethylsiloxane, 30 m × 0.25 mm i.d., film thickness 0.25 μm). The injector temperature was set at 200 °C, and the oven temperature program was as follows: The temperature was increased from 40 °C (2 min), until it reached 280 °C at 20 °C min^{-1}, and held for a duration of 5 minutes. Helium was utilized as the carrier gas at a flow rate of 1 mL min^{-1}.

2.4. General procedure for the homocoupling of arylboronic acids

Arylboronic acid (1.0 mmol) and Cu(I)-HAp catalyst (50 mg)

were introduced into a reaction vessel containing a suitable solvent, such as DMF (3 mL). The resultant mixture was stirred in air at room temperature for a period of 24 hours. Reaction progress was monitored using thin-layer chromatography (TLC). Upon completion of the reaction, the mixture was cooled and filtered to remove the catalyst. The filtrate was extracted with ethyl acetate, washed with brine, and dried over anhydrous Na_2SO_4. The solvent was then removed under reduced pressure, and the crude product was purified by column chromatography using n-hexane/ethyl acetate, yielding the biaryl products.

3. Results and Discussion

3.1. Characterization of HAp and Cu(I)-Hap

3.1.1 XRD analysis

The diffraction pattern of the HAp sample as illustrated in Fig. 2 exhibits the characteristic reflections of HAp at approximately 2θ = 25.9°, 28.1°, 29.2°, 31.9°, 33.1°, 34.2°, 39.8°, 46.8°, 49.6°, and 53.3°. The recent reflections are consistent with the hexagonal HAp phase, thereby confirming that the support has a well-defined crystalline structure corresponding to $Ca_{10}(PO_4)_6(OH)_2$ with space group $P6_3/m$. This finding is in agreement with PDF 98-002-6205 [40,46]. Following the impregnation process with CuI, most of the significant HAp reflections remain observable at similar 2θ positions in the Cu(I)-HAp sample. This finding indicates that the wet impregnation process did not disrupt the crystalline framework of the HAp support. New reflections at 2θ = 25.5°, 42.2°, and 49.9° correspond to the (111), (220), and (311) planes of cubic CuI. This finding indicates that the incorporation of crystalline CuI into the composite was successful. The strong reflection at 25.5° is of particular interest, as pure HAp typically exhibits its (002) reflection near 25.9°. The strong peak at 25.5° is presumably predominantly attributable to the CuI phase. Similarly, the reflection at 42.2° provides clear evidence for CuI incorporation as it is characteristic of CuI rather than pristine HAp. The peak observed at 49.9° is mainly attributable to CuI (311), although partial overlap with the HAp reflection near 49.5° may occur. The coexistence of CuI-related reflections and preserved HAp diffraction features demonstrates that the wet impregnation method has been successful in producing a Cu(I)-HAp composite while maintaining the structural integrity of the HAp support [47–50].

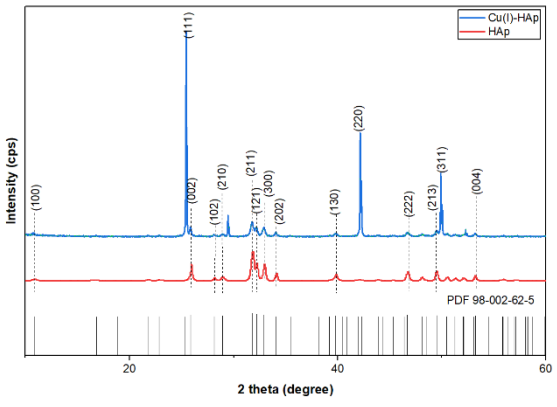

Fig. 2. X-ray diffractograms of HAp and Cu(I)-HAp

XRD results indicate the presence of crystalline CuI in the composite, yet this method alone is not capable of directly determining the oxidation state of copper. The presence of Cu(I) in the catalyst was identified through the utilization of CuI and diffraction peaks that matched the cubic CuI phase could be observed. The method for synthesizing Cu(I)-HAp in this study is similar to the approach utilized by Saha et al. [45], who synthesized made a CuI/HAp catalyst with a similar wet-impregnation process. In their work, ICP-MS and EDS confirmed the presence of copper in the hydroxyapatite support, and XPS results suggested the presence of Cu(I) species. Given the utilization of the same copper source, and a similar synthesis method, and observed CuI diffraction peaks, it is likely that Cu(I) species are present in our catalyst. However, the use of techniques sensitive to oxidation state, such as XPS, Auger spectroscopy, XANES, or EXAFS, was not employed, thus hindering the ability to ascertain the copper oxidation state with certainty. Therefore, the assignment of Cu(I) is an inference based on the evidence we have and previous studies, not definitive proof.

XRD analysis demonstrated that the crystallite size, calculated with the Scherrer equation, increased from 28.23 nm for HAp to 76.33 nm for Cu(I)-HAp. At the same time, crystallinity, measured as the ratio of the crystalline area to the total area, decreased from 82.40% to 48.86%. These results obtained from this study suggest that the addition of CuI did not result in the disruption of the main HAp phase but it did change its crystalline order.

The increase in crystallite size suggests the enlargement of the diffraction domains, while the decrease in crystallinity reflects increased local disorder arising from interactions between Cu species and the apatite matrix. A similar pattern has also been reported for Cu-modified HAp materials in which the primary apatite phase has been observed to be maintained despite a decrease in crystallinity following copper incorporation [46]. In addition, in the context of impregnated Cu-modified HAp catalysts, it has been demonstrated that the presence of Cu leads to alterations in the structural properties without eliminating the characteristic features of the support [49]. Therefore, the XRD data indicate that CuI was successfully deposited onto the HAp matrix without disrupting the support's main structure. The preservation of the HAp phase is important for maintaining the stability of the heterogeneous catalyst during the reaction [40,49].

3.1.2 FT-IR analysis

FT-IR analysis was conducted to examine the functional groups of HAp and Cu(I)-HAp and to complement the structural information obtained from XRD. As depicted in Fig. 3, the HAp spectrum exhibits characteristic PO_4^{3-} stretching vibrations in the 1100–1000 cm^{-1} region and phosphate bending modes near 560–600 cm^{-1}, thereby confirming the apatite framework. The presence of lattice hydroxyl groups is indicated by the presence of bands near 3570 cm^{-1} and the libration band at approximately 630 cm^{-1} [46,49,51,52].

A comparison with pure HAp indicates that the main phosphate and hydroxyl bands in the Cu(I)-HAp spectrum appear in similar regions. This observation suggests that the primary apatite framework remains largely unchanged following CuI impregnation. However, changes in band

intensity and slight shifts are observed, particularly in the phosphate-related regions at 1100–1000 and 600–560 cm^{-1}. These spectral changes suggest interactions between Cu(I) species and phosphate and/or hydroxyl groups on the HAp surface without any significant alteration to the main chemical structure of the support, a trend that has also been reported for Cu-modified HAp materials [49,51].

Furthermore, the absence of prominent carbonate bands in the regions of 1455-1410 and 880-870 cm^{-1}, indicating that, under typical conditions, CO_3^2 is not a dominant component in the samples [53]. The absence of strong organic bands in the 3000-2800 cm^{-1} region or near 1700 cm^{-1} suggests that most of the residual solvent, if any was present initially, was removed during the washing and drying processes. The findings from the FT-IR analysis are consistent with those from the XRD analysis, which indicated that the main crystalline phase of HAp remained unchanged after the addition of CuI. the combination of FT-IR and XRD data confirms the incorporation of CuI into the HAp matrix without compromising the key structural features of the HAp support.

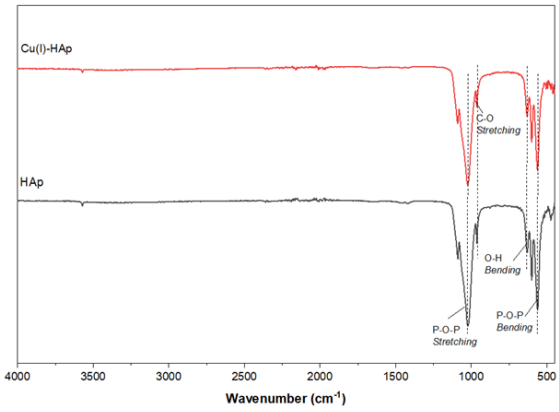

Fig. 3. FT-IR spectra of pure HAp and Cu(I)-HAp composite

3.1.3 SEM morphology

The comparison of the surface morphology of HAp and Cu(I)-HAp was conducted using SEM analysis. Additionally, the effect of CuI impregnation on the support structure was evaluated. This analysis is important for heterogeneous catalysts, given that morphological features such as particle shape, surface roughness, and agglomeration have the capacity to influence the exposure of surface sites, substrate–catalyst contact, and deposition of the active phase. As demonstrated in Fig. 4, the HAp sample consists of irregularly shaped particles that are interconnected to form larger aggregates with a relatively rough surface. Such agglomerated morphology is commonly observed in synthetic HAp, where primary particles tend to coalesce due to high surface energy and solid–solid interactions [40,54]. The rough and aggregated surface is relevant for catalytic applications by virtue of the fact that it can provide surface contact and anchoring sites for the deposition of active species on the support [40].

After modification to Cu(I)-HAp, the main morphology of the material was largely maintained, remaining as irregular particle aggregates with an agglomeration tendency similar to that of pristine HAp. However, analysis of the surface of the composite revealed a high degree of density, with fine particles appearing to be partially covering the surface. This finding indicates that the process of CuI loading occurred on the HAp surface without causing significant changes to the fundamental morphology of the support. This observation is consistent with previous reports indicating that metal incorporation into HAp does not always induce drastic morphological changes but may influence the surface state and the distribution of particle aggregates [46,53]. This interpretation is further supported by the EDS results, which indicate that the HAp sample exhibited the main constituent elements Ca, P, and O. In contrast, the Cu(I)-HAp sample exhibited additional Cu and I signals in conjunction with the HAp framework elements. The presence of Cu and I is indicative of the successful deposition of CuI species onto the HAp matrix. In this context, iodide is more appropriately regarded as part of the deposited CuI phase rather than as a constituent of the main HAp framework. The combined SEM–EDS results indicate that the modification proceeded through CuI deposition on the HAp surface while preserving the principal morphology of the support. From a catalytic viewpoint, such a structural feature is significant because the presence of the active phase at the solid interface may enhance substrate–catalyst contact while also contributing to the stability of the heterogeneous catalytic system during the reaction [12,49].

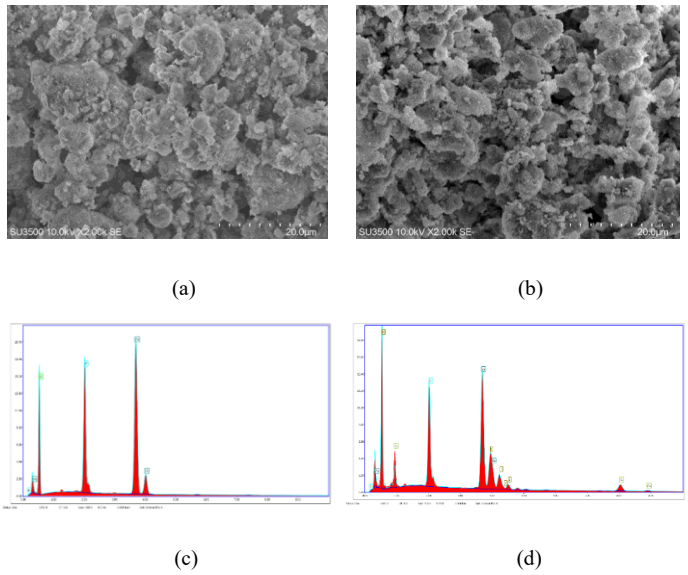

Fig. 4. Scanning electron micrographs of (a) HAp and (b) CuI-HAp, together with the corresponding EDS spectra of (c) HAp and (d) Cu(I)-HAp.

The characteristic FTIR, XRD, and SEM features of hydroxyapatite-based materials have also been reported by [55], including the presence of OH^- and PO_4^{3-} vibrations, crystalline HAp phases, and porous surface morphology. Consequently, the observed diffraction peaks, phosphate-related FTIR bands, and agglomerated porous morphology in the present catalyst are consistent with typical hydroxyapatite-based materials.

3.2. Optimization of homocoupling reaction conditions

The reaction conditions were optimized to evaluate the effects of solvent and atmosphere on the homocoupling of *p*-tolylboronic acid catalyzed by Cu(I)-HA. The results presented

in Table 1 demonstrate that the homocoupling of *p*-tolylboronic acid over the Cu(I)-HAp catalyst is strongly influenced by both the solvent system and the atmospheric conditions. The desired product, 4,4′-dimethylbiphenyl, was detected exclusively when dry DMF was utilized as the reaction medium and, to a lesser extent, in the dry DMF/DCM mixture. In contrast, wet DMF, H_2O, acetonitrile, and ethanol did not yield any detectable product under the conditions of the experiment. Amongst all reaction systems examined, dry DMF in air yielded the highest percentage of 80% (**entry 2**), followed by dry DMF under an O_2 atmosphere, which produced a yield of 76% (**entry 1**). These findings indicate that an anhydrous polar aprotic medium provides the most favorable environment for this catalytic system.

Table 1. Effect of solvent and reaction atmosphere on the Cu(I)–HAp-catalyzed homocoupling of *p*-tolylboronic acid.[a]

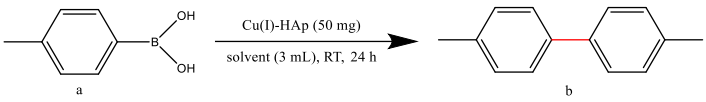

a b

Entry	Solvent	Reaction Atmosphere	Yield (%)
1	dry DMF	O_2	76
2	dry DMF	in air	80
3	wet DMF	O_2	-
4	wet DMF	in air	-
5	H_2O	O_2	-
6	H_2O	in air	-
7	Acetonitrile	O_2	-
8	Acetonitrile	in air	-
9	Ethanol	O_2	-
10	Ethanol	in air	-
11	dry DMF 2 eq/DCM	O_2	23
12	dry DMF 2 eq/DCM	in air	46

General conditions: a (1 mmol), Cu(I)-HAp (50 mg), solvent (3 mL), room temperature, 24 h. The isolated yields were determined after purification by column chromatography

The enhanced performance of dry DMF may be attributed to its capacity to maintain optimal substrate solubility, promote effective contact between *p*-tolylboronic acid and the catalyst surface, and preserve the active Cu species within a medium that does not significantly induce undesired changes in organoboron speciation. The lower yield observed in the dry DMF/DCM mixture suggests that the addition of DCM may reduce the effectiveness of the reaction medium, possibly by lowering the effective polarity of the solvent system and limiting mass-transfer efficiency. Conversely, the absence of detectable product in wet DMF, H_2O, and ethanol indicates that water or protic media may favor nonproductive pathways, including changes in boron speciation and protodeboronation [56], thereby suppressing the desired homocoupling reaction.

In addition to the solvent effect, the surface characteristics of HAp should also be considered, as this support may play a more active role in governing substrate interactions with Cu active sites. The HAp surface contains basic sites that are associated with OH^- groups and phosphate oxygen atoms. There are in combination with acidic sites including POH groups and Lewis-acidic Ca^{2+} centers. The presence of these acidic sites means that acid–base pairs can be generated on the material surface [41,57]. In the Cu(I)-HAp system, these surface functionalities may reasonably facilitate substrate adsorption and modulate substrate interaction with the Cu active centers [58]. In contrast, the HAp support has been demonstrated to contribute to the dispersion and stabilization of Cu species on the surface [49,59]. Collectively, these effects are likely to support the formation of the homocoupling product under mild aerobic conditions.

The screening results indicate that the catalytic performance of Cu(I)-HAp is governed not only by the presence of CuI as the active phase, but also by the compatibility between the solvent environment and the surface properties of the HAp support. It is evident that the most favorable balance for substrate solubilization, catalyst–substrate interaction, and preservation of the active catalytic species is achieved by dry DMF under air. Nevertheless, further verification is required concerning the specific role of the acid–base sites of HAp in the reaction pathway through more direct characterization of surface acidity and basicity, for example, by NH_3-TPD, CO_2-TPD, or probe-molecule FT-IR studies [30,34,41,49,60].

The atmospheric condition also played an important role in determining the catalytic performance of the Cu(I)-HAp system. In the two productive solvent systems, namely dry DMF and dry DMF/DCM, reactions performed in air consistently yielded higher product yields than those conducted under a pure O_2 atmosphere. This result indicates that atmospheric oxygen is sufficient to sustain the catalytic cycle, while the use of pure O_2 does not provide an additional beneficial effect. This interpretation is consistent with several reports on copper-based homocoupling of arylboronic acids that proceed efficiently under air exposure, including systems employing CuCl, Cu/1,10-phenanthroline complexes, and heterogeneous Cu-based catalysts such as HKUST-1 and CuI-zeolite [30,34,41,49,60].

Table 2. Optimization of catalyst amount and reaction time on reaction yield

Entry	Catalyst amount of Cu(I)-HAp	Reaction time	Yield (%)
1	50 mg	24 h	80
2	75 mg	24 h	73
3	100 mg	24 h	73
4	50 mg	6 h	66
5	50 mg	15 h	72

General conditions: *p*-tolylboronic acid (1 mmol), dry DMF (3 mL), in air. The isolated yields were determined after purification by column chromatography

The results presented in Table 2 demonstrate that the catalytic performance of Cu(I)-HAp was significantly determined by the amount of catalyst and reaction time. The optimization study revealed that 50 mg of CuI-HAp at room temperature for 24 h afforded the highest yield of the desired biaryl product (80.00%, Entry 1). Increasing the catalyst amount to 75 mg and 100 mg led to slightly lower yields of 73.30% and 72.97%, respectively, suggesting that excess catalyst did not improve the catalytic performance. This phenomenon may be associated with the increasing presence of aggregated particles within the heterogeneous system as evidenced by the SEM image (Fig. 4). The effect of reaction

time was also evaluated using 50 mg of Cu(I)-HAp.

The reduction in reaction time from 24 hours to 6 hours resulted in a yield of 66% (Entry 4), thereby demonstrating that an extended reaction duration is necessary for higher conversion. An increase in the reaction time to 15 hours improved the yield to 72% (Entry 5); however, this figure remained lower than the yield achieved after 24 hours. Therefore, the optimal condition was identified as 50 mg of Cu(I)-HAp for 24 hours, which provided the highest yield of 80%. The highest yield was observed after 24 hours, confirming that this reaction time was optimal among the conditions tested. The lower yields observed under less favorable conditions may be attributed to competing protodeboronation of the arylboronic acid, which could reduce the formation of the desired coupling product [68]. It was determined that the most effective reaction conditions were as follows; 50 mg of catalyst, room temperature, and 24 hours.

From a mechanistic perspective, the effect of the reaction atmosphere may be associated with the transmetalation and oxidation steps commonly proposed for Cu-mediated aerobic homocoupling of arylboronic acids. As demonstrated in literature reports, the catalytic process is generally suggested to involve B-to-Cu transmetalation, a process which generates aryl–Cu intermediates. These intermediates are then subject to oxidation of copper species under aerobic conditions.

However, these elementary steps were not directly investigated in the present study. The comparable performance obtained under open-air conditions relative to an O_2 atmosphere suggests that the role of oxygen is system-dependent, and that the use of pure O_2 does not necessarily enhance catalytic efficiency [38]. In this system, atmospheric oxygen appears to be sufficient to sustain catalytic turnover under the optimized conditions. It has been hypothesized that electron-rich arylboronic acids may be susceptible to competing oxidative pathways in some Cu-based reactions. However, the CuI-HAp catalyst still afforded a high yield for p-tolylboronic acid under open-air conditions. In addition, the acid–base surface properties of hydroxyapatite, particularly surface hydroxyl and phosphate groups, could plausibly assist substrate adsorption and activation, thereby facilitating the coupling process. Nevertheless, given the absence of dedicated mechanistic experiments were performed, the precise roles of oxygen, copper redox transformations, and HAp surface sites remain tentative and are discussed here based on literature precedents. Consequently, the optimal performance observed in dry DMF aerobic condition can be rationalized by the synergy of an anhydrous reaction medium, the surface properties of HAp, and sufficient aerobic oxidation under open-air conditions [37-38].

In considerations of the aforementioned factors and in accordance with relevant literature,[37,38] a plausible catalytic pathway for the CuI-HAp-catalyzed aerobic homocoupling of arylboronic acids is proposed in Scheme 1. Firstly, Cu(I)-HAp undergoes oxidation in the presence of O_2, which is followed by transmetalation with two molecules of arylboronic acid. These are activated through interaction with oxygen atoms on the HAp surface, resulting in HAp-Cu(III)$(Ar)_2$ (Scheme 1, Step 1). Subsequent reductive elimination releases the homocoupling product and regenerates the active Cu(I)-HAp catalyst (Fig. 5, Step 2).

It is imperative to note that the optimization study in the present work was limited to the selection of solvent and the consideration of atmospheric conditions. Consequently, the reaction conditions identified herein represent the most favorable conditions among those investigated rather than a comprehensive global optimum. It is acknowledged that further investigation is required to examine other potentially important variables, including catalyst loading, Cu loading, reaction temperature, reaction time, and substrate concentration. These variables may also influence catalytic performance. Future studies will focus on a more extensive optimization of these parameters to establish the full operational window of the CuI-HAp catalytic system.

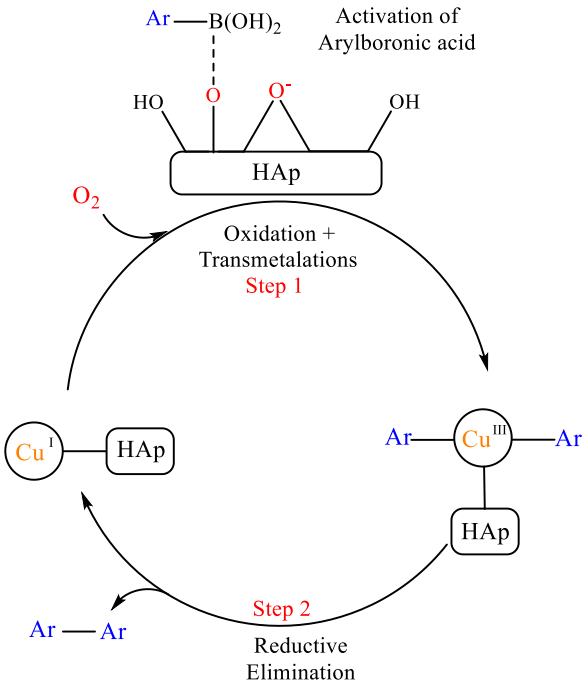

Fig. 5. Plausible reaction mechanism for CuI-HAp-catalyzed aerobic homocoupling of arylboronic acids

Product formation under the optimum conditions was further confirmed by GC, GC–MS, ^{1}H NMR, and ^{13}C NMR analyses (see Fig. 6). The GC chromatogram exhibited a single dominant peak at t_R = 10.77 min, indicating optimal reaction selectivity towards one major product. The corresponding GC–MS spectrum showed a molecular ion at *m/z* 182, which is consistent with the molecular formula $C_{14}H_{14}$ and the molecular weight of 4,4′-dimethylbiphenyl as reported in the NIST Chemistry WebBook. This structural assignment was further supported by the ^{1}H NMR spectrum, which exhibited two sets of aromatic signals at δ 7.45–7.36 and 7.18–7.09, together with a singlet at δ 2.30 attributable to two equivalent methyl groups. The ^{13}C NMR spectrum also demonstrated only five main signals at δ 138.31, 136.66, 129.45, 126.82, and 21.08, consistent with the high symmetry of a *para,para′*-disubstituted biphenyl framework. Collectively, these chromatographic and spectroscopic data confirm that the major product formed under the optimum conditions was 4,4′-dimethylbiphenyl. Furthermore, the obtained spectral features are in good agreement with literature reports on the homocoupling of arylboronic acids [31,37]. The findings indicate that the optimal conditions yielded the highest yield, and selectively directed the reaction towards the desired homocoupling product.

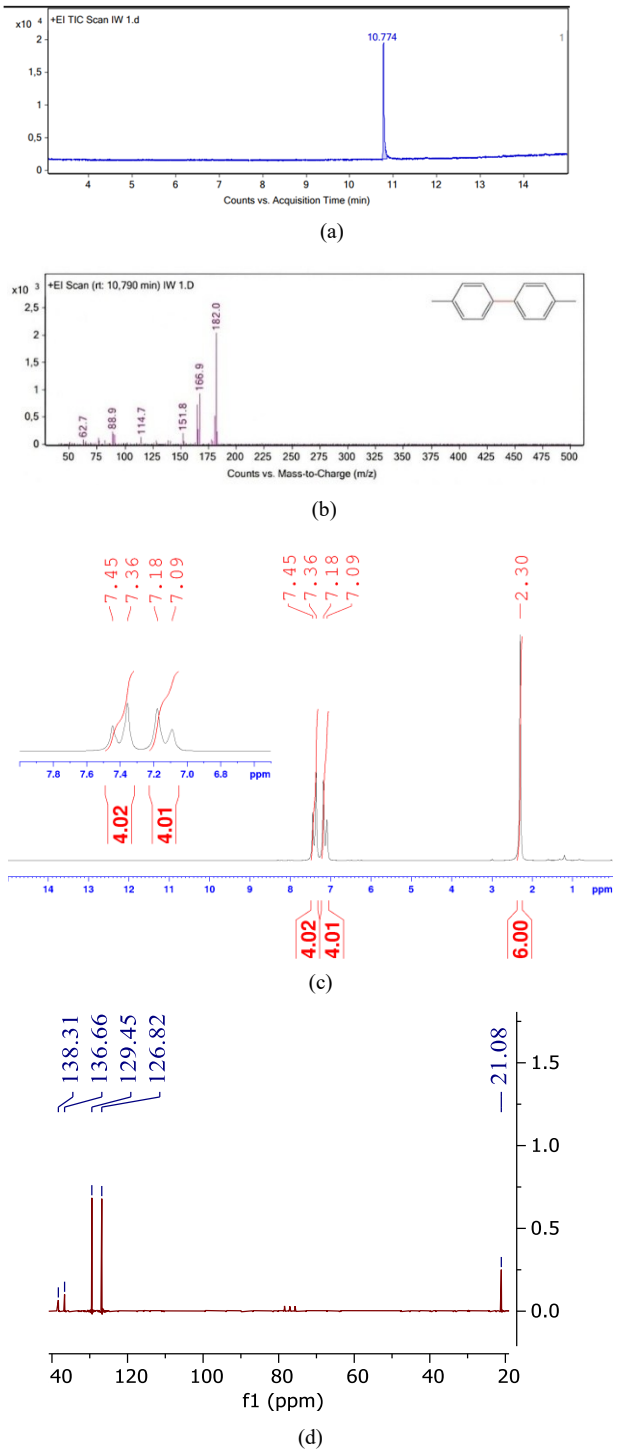

Fig. 6. (a) GC chromatogram of the homocoupling product; (b) GC–MS spectrum of the product; (c) ^{1}H NMR spectrum of 4,4′-dimethylbiphenyl; and (d) ^{13}C NMR spectrum of 4,4′-dimethylbiphenyl.

3.3. Reusability and structural stability

In view of the preceding optimization results, which demonstrated that the homocoupling of *p*-tolylboronic acid yielded the most optimal yield utilizing the Cu(I)-HAp catalyst in dry DMF under air at room temperature for a 24-hour period, the subsequent investigation focused on evaluating the reusability and structural stability of the catalyst. Each catalytic cycle was performed in triplicate, and the yields are expressed as the mean ± standard deviation. As demonstrated in Fig. 7, Cu(I)-HAp retained reasonable catalytic activity following repeated use, though the yield showed a gradual decrease from 78.19 ± 1.56% in the first cycle to 71.56 ± 0.58%, 58.44 ± 1.76%, and 53.53 ± 1.04% in the second, third, and fourth cycles, respectively. This trend indicates that the catalyst did not undergo rapid deactivation but rather experienced a progressive loss of efficiency over successive reaction cycles. For this heterogeneous Cu(I)-HAp catalyst, such behavior suggests that the material remains sufficiently stable for reuse, although some active sites may become less accessible after repeated catalytic runs.

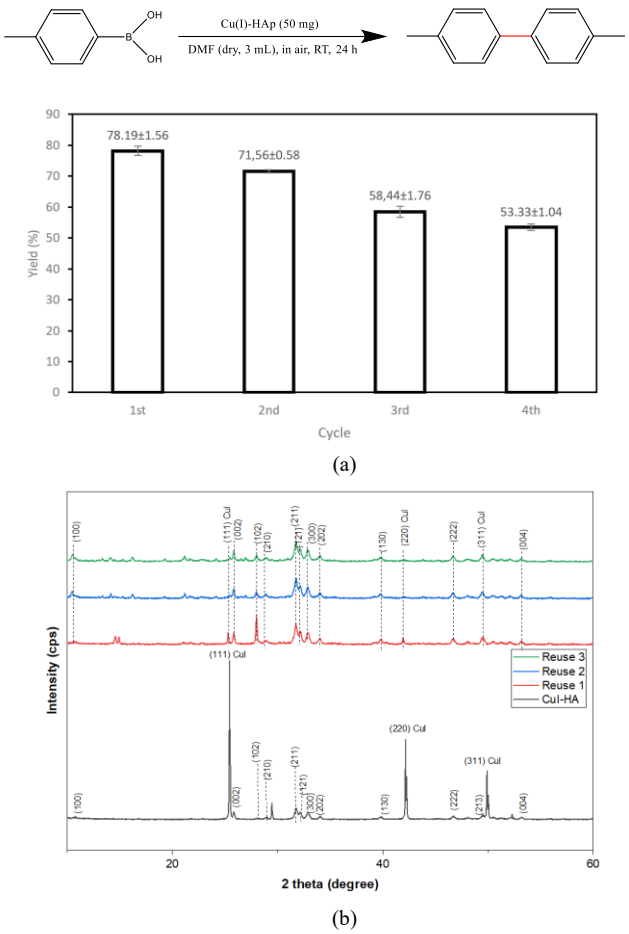

Fig. 7. (a) Cu(I)-HAp recyclability on reaction with a condition as stated in Table 1, entry 2; (b) XRD spectra of the recycled Cu(I)-HAp

In heterogeneous catalysis, the decrease in activity after repetitive use is commonly associated with poisoning, fouling, sintering or ageing, attrition or crushing, and partial leaching of active components during separation and washing processes, all of which are recognized as major deactivation pathways in solid catalysts [61,62]. In Cu-based catalytic systems, leaching and fouling have also frequently been reported as key factors responsible for the loss of activity after several reuse cycles [63]. Consequently, the gradual decrease in yield observed for CuI-HAp may be associated with alterations in the active surface sites, as opposed to the complete structural degradation of the material. The following factors may be contributing factors to the issues: fouling by reaction residues, partial blockage of catalytic sites, catalyst loss during recovery, or partial leaching of copper species. However, these possibilities were not the subject of direct investigation in the present study.

In the case of metal-modified HAp catalysts, the decline in

catalytic performance after reuse is commonly attributable to a reduced number of exposed active phases, blockage of catalytic sites by organic residues, or partial catalyst loss during the recovery process. In contrast, the HAp framework generally remains stable as a support [64,65]. Accordingly, the observed decrease in activity is consistent with gradual catalyst deactivation, though the dominant deactivation pathway cannot be conclusively determined without any additional post-reaction characterization. This finding suggests that Cu(I)-HAp still exhibits acceptable reusability for practical catalytic application, although its stability is not yet sufficient to fully maintain the initial activity over successive reaction cycles [12,40,49,64].

The XRD patterns of the fresh catalyst and the catalyst after three reuse cycles still exhibited the characteristic reflections of HAp at relatively consistent 2θ positions, without the appearance of any dominant new crystalline phase. The absence of significant loss of the main HAp reflections or major structural changes indicates that no substantial degradation of the bulk support occurred during the reaction and recovery processes. Consequently, the crystalline framework of HAp can be regarded as being predominantly preserved after repeated utilization.

This interpretation is consistent with previous studies reporting the capacity of HAp-supported Cu systems to retain the phase stability of HAp after repeated catalytic cycles, while Cu species remain well dispersed on the support surface and the catalyst maintains reasonable activity [64,65]. Furthermore, studies on HAp-based catalysts for homocoupling reactions have demonstrated that modification of the support interface can preserve structural stability while supporting catalytic performance, as reported for the homocoupling of phenylboronic acid over modified HAp systems [64,65]. Therefore, the similarity of the XRD patterns before and after reuse confirms that the durability of the catalyst is primarily supported by the stability of the bulk HAp framework as opposed to significant changes in the primary crystalline phase.

When the reusability and XRD data are considered together, the moderate decrease in yield is most likely associated with changes on the catalyst surface rather than with degradation of the bulk support structure. This finding suggests that the observed decrease in activity may be attributed to a decrease in the number of exposed CuI active sites, which could be a consequence of fouling by reaction residues, partial blockage of the surface by adsorbed species, or minor Cu loss during the recovery process. Meanwhile, the HAp structure remains uncompromised, preserving its mechanical integrity.

The recyclability of CuI-HAp was evaluated under the optimized reaction conditions. It was found that the catalyst could be reused for several cycles, although a gradual decrease in catalytic activity was observed. This decline may be associated with the loss of active copper species during the recycling process. To further evaluate the stability of copper species on the hydroxyapatite support, the Cu content of the fresh and reused catalysts was analyzed by AAS after acid digestion of the solid samples. The fresh CuI-HAp catalyst contained 76 mg g^{-1} Cu, corresponding to 8 wt% Cu, whereas the reused catalyst contained 65 mg g^{-1} Cu, corresponding to 7 wt% Cu. The findings suggest that approximately 86% of the initial copper content was retained after reuse, while approximately 14% of Cu was lost during the recycling process. It can be hypothesized that the decrease in Cu content may be a contributing factor to the gradual decline in catalytic performance observed upon reuse. The retention of most of the copper content, in conjunction with the preserved hydroxyapatite structure as evidenced by XRD after reuse, suggests that the copper species remain reasonably associated with the HAp support during catalysis process. These findings are consistent with the behavior expected for a recyclable solid catalyst, suggesting that the catalytic process is predominantly heterogeneous. Accordingly, despite the recyclability, structural stability, and AAS analysis of the reused solid catalyst supporting the relative stability of CuI-HAp, the exclusive involvement of dissolved copper species cannot be completely excluded at this stage.

While XRD patterns demonstrate that the bulk hydroxyapatite framework remains largely unchanged after repeated use, XRD primarily detects crystalline structural changes and does not directly reveal surface composition, copper oxidation state, metal leaching, or the accumulation of adsorbed species. Consequently, the preservation of the diffraction pattern does not preclude surface-related deactivation processes. To identify the dominant deactivation mechanism, additional analyses would be required including SEM, EDS mapping, ICP measurements, and XPS characterization of the recovered catalyst.

Table 3. Comparison of catalytic performance of Cu(I)-HAp with representative homogeneous and heterogeneous catalysts for the homocoupling of arylboronic acid

Catalyst	Substrate	Condition	Yield (%)	Recycl.	Ref.
CuCl	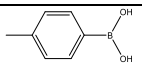	RT, air, 4 h	73	Homog.	[34]
Cu / Phenanthroline	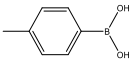	RT, air, 6 h	75	Homog.	[35]
Cu(I)-USY Zeolite	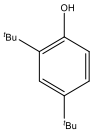	MeOH, 60°C, air, 22 h, Cs_2CO_3 base	70	3 cycles	[12]
HKUST-1	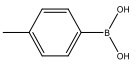	DMF, RT, O_2, 24 h	93	3 cycles	[37]
Pd-HAp	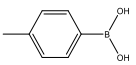	EtOH, 50°C, air, 24 h,	88	5 cycles	[31]
Cu(I)-HAp (this work)	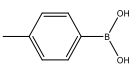	DMF, RT, O_2, 24 h	80	4 cycles	This work

This interpretation is consistent with the general principles of heterogeneous catalyst deactivation, in which performance loss is often governed by changes in surface chemistry even when the bulk diffraction pattern remains relatively unchanged [12,66]. In Cu-supported HAp systems, the relationship between support stability and sustained catalytic activity has also been reported, further supporting the role of HAp as a suitable support for heterogeneous Cu catalysts [64,65]. It is therefore evident that the results obtained demonstrate the function of CuI-HAp as a recyclable solid catalyst for biaryl synthesis whilst also maintaining its structural integrity over several reaction cycles. However, additional post-reaction

characterization would be required to identify the dominant catalyst deactivation pathway and to fully evaluate the extent of possible copper leaching. Nevertheless, further optimization is still required to suppress surface deactivation and improve the retention of catalytic activity over repeated reaction cycles [40,64,67].

Table 3 presents a comparison in the catalytic performance of the present Cu(I)-HAp catalyst with representative homogeneous and heterogeneous systems reported for arylboronic acid homocoupling. While HKUST-1 and Pd-HAp exhibit higher yields, Cu(I)-HAp offers advantages in terms of cost efficiency, material sustainability, and operational simplicity due to the utilization of an earth-abundant metal and a robust inorganic support. Moreover, the catalyst can be readily recovered and reused, thus making it a practical alternative to more complex or noble metal-based systems.

3.4. Substrate scope and product confirmation

Following the establishment of optimized conditions, namely dry DMF in air, the substrate scope was further evaluated using a series of substituted arylboronic acids to assess the generality of the Cu(I)-HAp catalyst. As depicted in Table 4, this catalytic system was capable of accommodating arylboronic acids bearing electron-donating and electron-withdrawing substituents, in addition to substituents located at the *ortho*, *meta*, and *para* positions. Nevertheless, the reaction efficiency was found to be highly dependent upon both the electronic nature and steric demand of the substituents.

Among the substrates examined, 4-*tert*-butylphenylboronic acid (**1f**) and 4-methylphenylboronic acid (**1c**) were found to afford the highest yields, with the corresponding homocoupling products being obtained in 83% (**2f**) and 80% (**2c**) yield, respectively. A satisfactory yield was also obtained from 4-bromophenylboronic acid (**1e**), which produced the desired biaryl product in 67% (**2e**) yield. In contrast, substrates with less favorable steric or electronic characteristics demonstrated markedly lower reactivity. For example, 2-methylphenylboronic (**1a**) acid and 3-methylphenylboronic acid (**1b**) yielded only trace amounts of product, while 2-methoxyphenylboronic acid (**1i**), 4-biphenylboronic acid (**1g**), and *trans*-2-phenylvinylboronic acid (**1h**) gave low to moderate yields.

This substrate-dependent behavior indicates that the Cu(I)-HAp catalyst possesses a reasonably broad substrate scope, although its catalytic performance is more favorable for arylboronic acids that are relatively less sterically hindered and electronically compatible with the Cu-mediated homocoupling pathway. It is evident that the higher yields observed for *para*-substituted substrates suggest that reduced steric congestion surrounding the boronic acid moiety may facilitate more effective interaction with the Cu active sites on the HAp surface. This interpretation is consistent with previous reports on copper-catalyzed homocoupling of arylboronic acids. In these earlier studies, it was demonstrated that Cu-based catalysts were able to tolerate various substituents, including halogens and electron-donating groups. Nevertheless, it was also found that the final reaction outcome remained highly dependent on the combined effects of substrate structure and catalyst properties [12,66].

When classified according to the substituent properties, *para*-alkyl electron-donating groups, as represented by the 4-methyl (**1c**) and 4-*tert*-butyl (**1f**) substituents, were clearly the most favorable in this catalytic system, whereas the 4-methoxy- (**1j**) substituted substrate afforded only a moderate yield of 47% (**2j**). This finding suggests that the electronic effect may not always be straightforwardly related to the strength of the electron-donating group, as a stronger electron-donating group does not necessarily lead to a higher yield. In the context of Cu-based catalysts under aerobic conditions, the moderate yield obtained from the 4-methoxy- (**1j**) substituted substrate may indicate that electron-rich substrates are reactive but can also be more susceptible to competing oxidative side pathways. This interpretation is consistent with reports on the HKUST-1 system, in which arylboronic acids bearing electron-donating substituents were found to compete with the formation of hydroxylated products when the reaction was conducted in air [37].

In contrast, halogenated substrates were still tolerated by the Cu(I)-HAp catalyst, although a clear difference was observed between the 4-bromo- (**1e**) and 4-fluoro- (**1d**) substituted substrates, which afforded yields of 67% (**2e**) and 41% (**2d**), respectively. The decline in yield might be attributable to protodeboronation, a phenomenon that has been observed in electron-poor aryl boronic acids. It has been established that substrates of aryl boronic acids bearing more electronegative substituents are more prone for protodeboronation [68].

The role of steric hindrance is most clearly reflected in the comparison of positional isomers. In the methyl-substituted series, a shift in the substituent position from *para* to *ortho* or *meta* resulted in a significant decline in yield, from 80% (**2c**) to only trace amounts of product. A similar trend was observed in the methoxy-substituted series, wherein 4-methoxyphenylboronic acid (**1j**) yielded a higher percentage than 2-methoxyphenylboronic acid (**1i**) (47% (**2j**) vs 25% (**2i**)). The results obtained indicate that *ortho* substitution is particularly unfavorable, a phenomenon that is likely attributable to its capacity to hinder substrate approach to the active Cu centers and/or to complicate the proper orientation of two aryl fragments during the C–C bond-forming step.

The low yields obtained from larger substrates, such as 4-biphenylboronic acid (**1g**) and *trans*-2-phenylvinylboronic acid (**1h**), further suggest that the extension of the π-conjugated framework or an increase in the effective substrate size can also limit the efficiency of the homocoupling process. The findings demonstrate that the Cu(I)-HAp catalyst exhibits good tolerance towards several classes of substituents but shows a clear preference for *para*-substituted substrates that are less sterically hindered. Such behavior is consistent with the nature of Cu-mediated homocoupling reactions, which are known to be highly efficient with less sterically hindered substrates [34,35,38].

Table 4. Scope of arylboronic acids in the Cu(I)-HAp-catalyzed homocoupling reaction

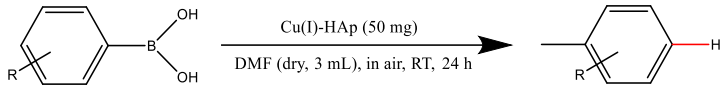

Entry	Arylboronic acid substrate[a]	Product[b]	Yield (%)	Characterization
1	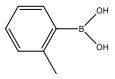 1a	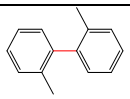 2a	Trace	-
2	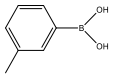 1b	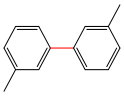 2b	Trace	-
3	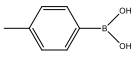 1c	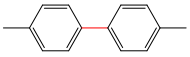 2c	80	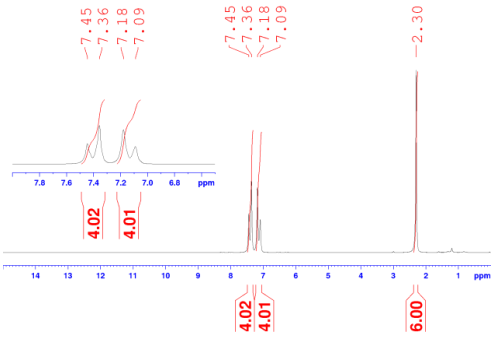 2c ^{1}H NMR (91 MHz, $CDCl_3$) δ 7.45–7.36 (d, 4H), 7.18–7.09 (d, 4H), 2.30 (s, 6H). The spectroscopic data were consistent with those reported in the literature [12,34,37,66].
4	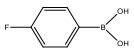 1d	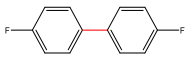 2d	41	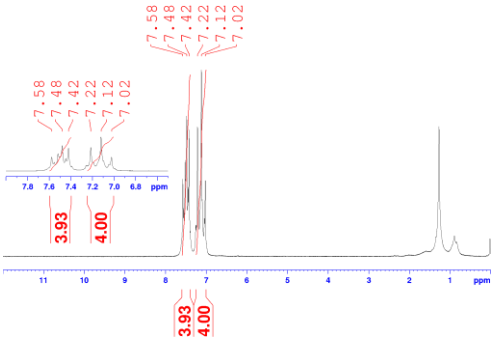 2d ^{1}H NMR (91 MHz, $CDCl_3$) δ 7.58–7.42 (d, 4H), 7.22–7.02 (d, 4H). The spectroscopic data were consistent with those reported in the literature [12,37,66].

Table 4 (continued). Scope of arylboronic acids in the Cu(I)-HAp-catalyzed homocoupling reaction

Entry	Arylboronic acid substrate[a]	Product[b]	Yield (%)	Characterization
5	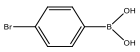 1e	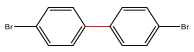 2e	67	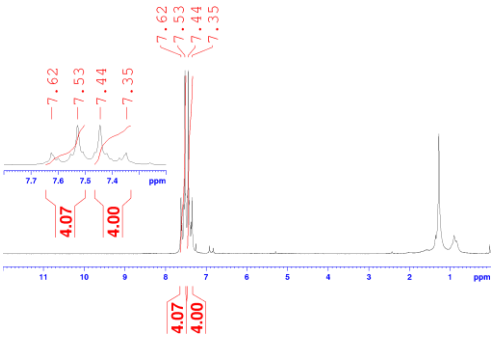 2e ^{1}H NMR (91 MHz, $CDCl_3$) δ 7.62 – 7.53 (m, 4H), 7.44 – 7.35 (m, 4H). The spectroscopic data were consistent with those reported in the literature [34,37,66].
6	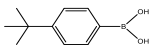 1f	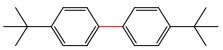 2f	83	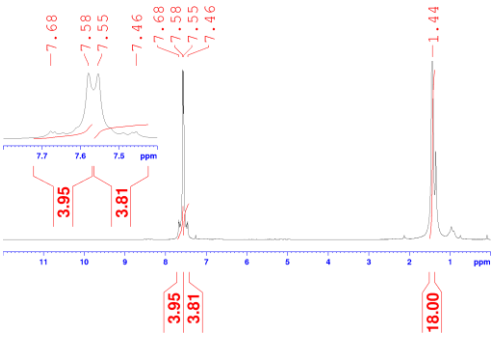 2f ^{1}H NMR (91 MHz, $CDCl_3$) δ 7.68–7.48 (m, 8H), 1.44 (s, 18H). The spectroscopic data were consistent with those reported in the literature [34,37].
7	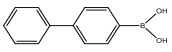 1g	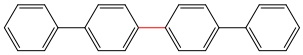 2g	29	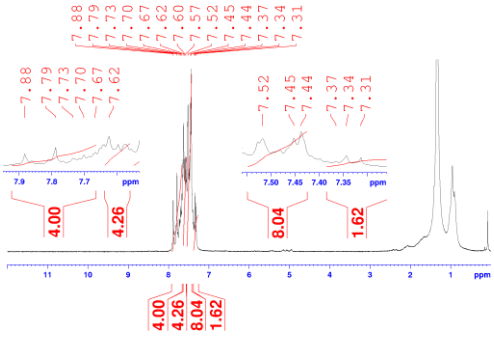 2g ^{1}H NMR (91 MHz, $CDCl_3$) δ 7.88–7.62 (m, 8H, Ar–H), 7.52–7.31 (m, 10H, Ar–H). The spectroscopic data were consistent with those reported in the literature [69].

Table 4 (continued). Scope of arylboronic acids in the Cu(I)-HAp-catalyzed homocoupling reaction

Entry	Arylboronic acid substrate[a]	Product[b]	Yield (%)	Characterization
8	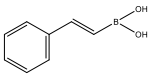 1h	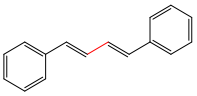 2h	37	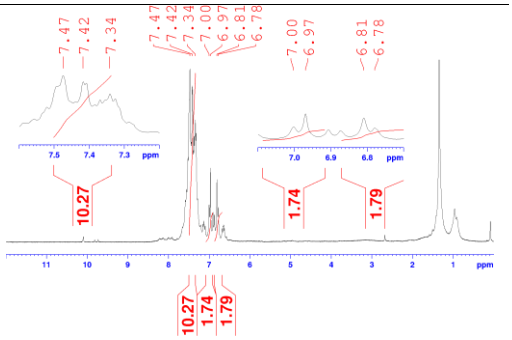 2h ^{1}H NMR (91 MHz, $CDCl_3$) δ 7.47–7.34 (m, 10H), 7.00–6.78 (m, 4H). The spectroscopic data were consistent with those reported in the literature [70].
9	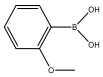 1i	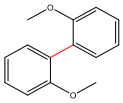 2i	25	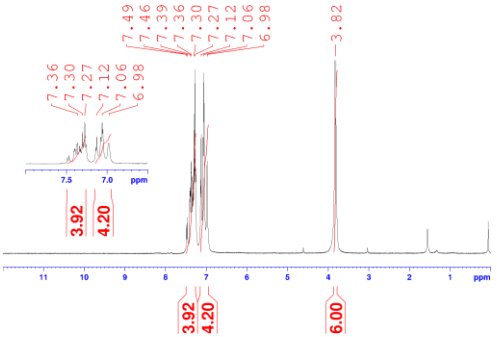 2i ^{1}H NMR (91 MHz, $CDCl_3$) δ 7.36 – 7.27 (m, 4H), 7.12 – 6.98 (*m*, 4H), 3.82 (*s*, 6H). The spectroscopic data were consistent with those reported in the literature [12,37].
10	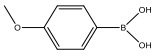 1j	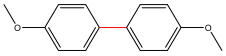 2j	47	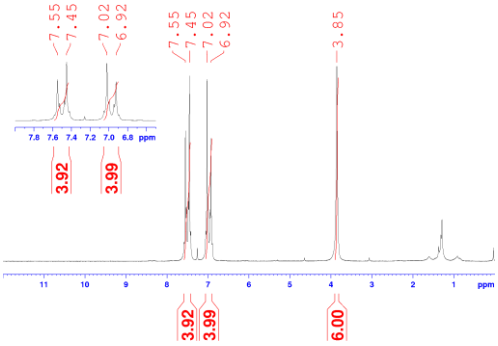 2j ^{1}H NMR (91 MHz, $CDCl_3$) δ 7.55 – 7.45 (*m*, 4H), 7.02 – 6.92 (*m*, 4H), 3.85 (*s*, 6H). The spectroscopic data were consistent with those reported in the literature [12,37,66].

General conditions: [a] (1 mmol), Cu(I)-HAp (50 mg), solvent (3 mL), in air, room temperature, 24 h. The isolated yields were determined after purification by column chromatography

When the relationship between substrate scope and selectivity is considered holistically, the most reactive substrates in this catalytic system are *para*-substituted arylboronic acids bearing alkyl substituents, particularly 4-*tert*-butylphenylboronic acid (**1f**) and 4-methylphenylboronic acid (**1c**). The electron-rich nature of these substrates is conducive to the formation of aryl–Cu intermediates, while being less susceptible to competing oxidative side pathways in comparison to substrates bearing stronger electron-donating groups renders them favorable. In contrast, the low yields observed for *ortho*-substituted isomers indicate that steric hindrance has a pronounced effect on the C–C bond-forming process. Meanwhile, the moderate to low yields obtained for several other substrates suggest that an increase in substituent size or changes in electronic character can reduce the efficiency of the homocoupling pathway.

Consequently, the Cu(I)-HAp system can be regarded as having considerable practical utility for a range of substituted arylboronic acids. However, its effectiveness is governed by the balance between steric accessibility to the active Cu centers and the electronic tendency of the substrate to undergo a productive homocoupling pathway. It is evident from literature on Cu-based MOF, CuCl, and Cu-zeolite catalytic systems that the generality of arylboronic acid homocoupling is achieved because the catalyst is able to maintain the dominant homocoupling pathway across a reasonably broad substrate range [12,34,66].

4. Conclusion

The Cu(I)-HAp composite has been successfully developed as a heterogeneous catalyst for the aerobic homocoupling of arylboronic acids under mild conditions, with a high degree of success. Structural and morphological characterization by XRD, FT-IR, and SEM–EDS confirmed the successful deposition of CuI on the HAp support while preserving the main crystalline framework and morphology of HAp. The catalytic study revealed that the reaction was highly sensitive to the solvent system and atmospheric condition, with dry DMF in air at room temperature for 24 hours providing the optimum conditions and affording 4,4′-dimethylbiphenyl in approximate yield of 80%. The catalyst demonstrated reasonable reusability over four cycles, although a gradual decrease in yield was observed. The similarity of the XRD patterns before and after reuse indicates that this loss of activity is more likely associated with surface deactivation than with collapse of the bulk HAp structure. Substrate scope evaluation further demonstrated that Cu(I)-HAp is applicable to a range of substituted arylboronic acids, with the best performance observed for less sterically hindered *para*-substituted substrates. The findings of this study highlight Cu(I)-HAp as a promising reusable heterogeneous catalyst for the operationally simple aerobic biaryl synthesis.

Acknowledgements

The authors would like to express their gratitude to the Pusat Pembiayaan Pendidikan Tinggi (BPPT) Kemendikbudristek through the Beasiswa Pendidikan Indonesia (BPI), and the Lembaga Pengelola Dana Pendidikan (LPDP) and Doctoral Dissertation Research (Penelitian Disertasi Doktor) Kemdiktisaintek 2026, No.100/C3/DT/05.00/PL-MULTITAHUNLANJUTAN/2026 and 1729/UN6.3.1/PT.00/2026

Credit author statement

Iis Intan Widiyowati: Conceptualization, Methodology, Supervision, Writing–Original Draft, Project Administration, Funding Acquisition.
Atiek Rostika Noviyanti: Data Curation, Investigation, Validation, Writing–Review & Editing.
Yudha Prawira Budiman: Data Curation, Resources, Visualization, Writing–Review & Editing.
Mukhamad Nurhadi: Formal Analysis, Investigation, Writing–Review & Editing.
Muhamad R. S. Sidik: Writing–Review & Editing
Muhammad R. Ramadhan: Writing–Review & Editing

References

1. D. Pal, P. Sahu, G. Sethi, C. E. Wallace and A. Bishayee, *Gossypol and Its Natural Derivatives: Multitargeted Phytochemicals as Potential Drug Candidates for Oncologic Diseases*, Pharmaceutics. 14 (2022) 2624.
2. G. Bringmann, C. Günther, M. Ochse, O. Schupp and S. Tasler, *Biaryls in Nature: A Multi-Facetted Class of Stereochemically, Biosynthetically, and Pharmacologically Intriguing Secondary Metabolites*, Fortschr. Chem. Org. Naturst. 82 (2001) 1–249.
3. J. B. McMahon, M. J. Currens, R. J. Gulakowski, R. W. Buckheit Jr., C. Lackman-Smith, Y. F. Hallock, et al., *Michellamine B, a Novel Plant Alkaloid, Inhibits Human Immunodeficiency Virus-Induced Cell Killing by at Least Two Distinct Mechanisms*, Antimicrob. Agents Chemother. 39 (1995) 484–488.
4. G. M. Cragg, D. J. Newman and D. G. I. Kingston, *Terrestrial Plants as a Source of Novel Pharmaceutical Agents*, Compr. Nat. Prod. II. 2 (2010) 5–39.
5. J. Xu and H. Xu, *Magnolol: Chemistry and biology*, Ind. Crops Prod. 205 (2023) 117493.
6. J. Zhang, Z. Chen, X. Huang, W. Shi, R. Zhang, M. Chen, et al., *Insights on the Multifunctional Activities of Magnolol*, BioMed Res. Int. 2019 (2019) 1847130.
7. S. Yuan, J. Chang and B. Yu, *Construction of Biologically Important Biaryl Scaffolds through Direct C–H Bond Activation: Advances and Prospects*, Top. Curr. Chem. 378 (2020) 21.
8. S. Y. Dai, W. X. Qin, S. Yu, C. Li, Y. H. Yang and Y. H. Pei, *Honokiol and magnolol: A review of structure-activity relationships of their derivatives*, Phytochemistry 223 (2024) 114132.
9. X. Li, Z. Yuan, Y. Wang, W. Wang and J. Shi, *Recent advances of honokiol: pharmacological activities, manmade derivatives and structure-activity relationship*, Eur. J. Med. Chem. 272 (2024) 116471.
10. *M. Faysal, J. Khan, M. Zehravi, N. Nath, L. P. Singh, S. Kakkar, et al., Neuropharmacological potential of honokiol and its derivatives from Chinese herb Magnolia species: understandings from therapeutic viewpoint*, Chin. Med. 18 (2023) 152.
11. H. Yang and W. Tang, *Enantioselective construction of ortho-sulfur- or nitrogen-substituted axially chiral biaryls and asymmetric synthesis of isoplagiochin D*, Nat. Commun. 13 (2022) 4392.

12. X. Di, T. Garnier, A. Clerc, E. Jung, C. Lherbet, V. Bénéteau, et al., *CuI-Zeolite Catalysis for Biaryl Synthesis via Homocoupling Reactions of Phenols or Aryl Boronic Acids*, Molecules 29 (2024) 5552.
13. F. Medici, S. Resta, A. Puglisi, S. Rossi, L. Raimondi and M. Benaglia, *Electrochemical organic synthesis of electron-rich biaryl scaffolds: An update*, Molecules 26 (2021) 6968.
14. H. Shimizu, I. Nagasaki and T. Saito, *Recent advances in biaryl-type bisphosphine ligands*, Tetrahedron 61 (2005) 5405–5432.
15. S. Akutagawa, *Asymmetric synthesis by metal BINAP catalysts*, Appl. Catal. A Gen. 128 (1995) 171–207.
16. S. B. Tsogoeva, *Privileged Brønsted acid organocatalysis*, Nat. Catal. 7 (2024) 7–9.
17. A. Zamfir, S. Schenker, M. Freund and S. B. Tsogoeva, *Chiral BINOL-derived phosphoric acids: Privileged Brønsted acid organocatalysts for C-C bond formation reactions*, Org. Biomol. Chem. 8 (2010) 5262–5276.
18. J. W. Goodby, *4'-pentyl-4-cyanobiphenyl - 5CB*, Liq. Cryst. 51 (2024) 1272–1295.
19. G. Pathak, B. Phettong and N. Chattham, *Optimization of 4-Cyano-4'-pentylbiphenyl Liquid Crystal Dispersed with Photopolymer: Application Towards Smart Windows and Aerospace Technology*, Polymers 17 (2025) 2232.
20. N. Y. Canli, H. Ocak, S. Ozturk, B. Bilgin Eran, S. Ozbey, D. Güzeller, et al., *Determination of dielectric properties of 5CB nematic liquid crystal doped with new chiral calamitic compounds*, J. Mater. Sci. Mater. Electron 34 (2023) 1335.
21. D. Devadiga and T. N. Ahipa, *A review on the emerging applications of 4-cyano-4'-alkylbiphenyl (nCB) liquid crystals beyond display*, Mater. Sci. Eng. B 275 (2022) 115522.
22. A. Y. Choi, T. Yamaguchi and C. H. Han, *A photochemical investigation into operational degradation of arylamines in organic light-emitting diodes*, Res. Chem. Intermed. 39 (2013) 1571–1579.
23. S. Inanlou, R. Cortés-Mejía, A. D. Özdemir, S. Höfener, W. Klopper, W. Wenzel, et al., *Understanding excited state properties of host materials in OLEDs: Simulation of absorption spectrum of amorphous 4,4-bis(carbazol-9-yl)-2,2-biphenyl (CBP)*, Phys. Chem. Chem. Phys. 24 (2022) 4576–4587.
24. T. Zhang, Y. Liang, J. Cheng and J. Li, *A CBP derivative as bipolar host for performance enhancement in phosphorescent organic light-emitting diodes*, J. Mater. Chem. C. 1 (2013) 757–764.
25. K. Chen, G. He and Q. Tang, *Air and moisture stable robust bio-polymeric palladium catalyzed CC bond formation and its application to the synthesis of fungicidal*, J. Ind. Eng. Chem. 124 (2023) 165–174.
26. A. Drageset, V. Elumalai and H.-R. Bjørsvik, *Synthesis of Boscalid via a three-step telescoped continuous flow process implemented on a MJOD reactor platform*, React. Chem. Eng. 3 (2018) 550–558.
27. L. E. Zetzsche, J. A. Yazarians, S. Chakrabarty, M. E. Hinze, L. A. Murray, A. L. Lukowski, et al., *Biocatalytic oxidative cross-coupling reactions for biaryl bond formation*, Nature 603 (2022) 79–85.
28. H. D. Gurupadaswamy, V. L. Ranganatha, R. Ramu, S. M. Patil and S. A. Khanum, *Competent synthesis of biaryl analogs via asymmetric Suzuki–Miyaura cross-coupling for the development of anti-inflammatory and analgesic agents*, J. Iran. Chem. Soc. 19 (2022) 2421–2436.
29. J. Hassan, M. Sévignon, C. Gozzi, E. Schulz and M. Lemaire, *Aryl–Aryl Bond Formation One Century after the Discovery of the Ullmann Reaction*, Chem. Rev. 102 (2002) 1359–1470.
30. A. J. J. Lennox and G. C. Lloyd-Jones, *Selection of boron reagents for Suzuki–Miyaura coupling*, Chem. Soc. Rev. 43 (2014) 412–443.
31. D. P. Novianti, M. Rashifari, M. R. Ramadhan, I. I. Widiyowati, P. K. Salsabila, A. W. Waardhani, et al., *Homocoupling reaction of p-tolylboronic acid with palladium-hydroxyapatite composite from chicken eggshell as the catalyst*, Results Chem. 15 (2025) 102297.
32. S. N. S. Vasconcelos, J. S. Reis, I. M. de Oliveira, M. N. Balfour and H. A. Stefani, *Synthesis of symmetrical biaryl compounds by homocoupling reaction*, Tetrahedron 75 (2019) 1865–1959.
33. F. Ullmann and J. Bielecki, *Ueber Synthesen in der Biphenylreihe*, Ber. Dtsch. Chem. Ges. 34 (1901) 2174–2185.
34. G. Cheng and M. Luo, *Homocoupling of arylboronic acids catalyzed by CuCl in air at room temperature*, Eur. J. Org. Chem. 2011 (2011) 2519–2523.
35. N. Kirai and Y. Yamamoto, *Homocoupling of arylboronic acids catalyzed by 1,10-phenanthroline-ligated copper complexes in air*, Eur. J. Org. Chem. 2009 (2009) 1864–1867.
36. J. R. Falck, S. Mohapatra, M. Bondlela and S. K. Venkataraman, *Homocoupling of alkyl-, alkenyl-, and arylboronic acids*, Tetrahedron Lett. 43 (2002) 8441–8443.
37. Y. P. Budiman, M. Rashifari, S. Azid, I. Z. Ghafara, Y. Deawati, Y. Permana, et al., *HKUST-1-Catalyzed Homocoupling of Arylboronic Acids*, ChemistrySelect 9 (2024) e202304913.
38. A. Salamé, J. Rio, I. Ciofini, L. Perrin, L. Grimaud and P. A. Payard, *Copper-Catalyzed Homocoupling of Boronic Acids: A Focus on B-to-Cu and Cu-to-Cu Transmetalations*, Molecules 27 (2022) 7517.
39. D. Pham Minh, *Introduction to Hydroxyapatite-based Materials in Heterogeneous Catalysis*, in: Design and Applications of Hydroxyapatite-Based Catalysts, Wiley-VCH, Weinheim, 2022, pp. 1–18.
40. A. Fihri, C. Len, R. S. Varma and A. Solhy, *Hydroxyapatite: A review of syntheses, structure and applications in heterogeneous catalysis*, Coord. Chem. Rev. 347 (2017) 48–76.
41. S. Diallo-Garcia, M. B. Osman, J. M. Krafft, S. Casale, C. Thomas, J. Kubo, et al., *Identification of surface basic sites and acid-base pairs of hydroxyapatite*, J. Phys. Chem. C 118 (2014) 12744–12757.
42. D. Saha, T. Chatterjee, M. Mukherjee and B. C. Ranu, *Copper(I) hydroxyapatite catalyzed sonogashira reaction of alkynes with styrenyl bromides*, J. Org. Chem. 77 (2012) 9379–9383.
43. B. M. Choudary, C. Sridhar, M. L. Kantam and B. Sreedhar, *Hydroxyapatite supported copper catalyst for effective three-component coupling*, Tetrahedron Lett. 45 (2004) 7319–7321.
44. A. R. Noviyanti, N. Akbar, Y. Deawati, E. E. Ernawati, Y. T. Malik, R. P. Fauzia, et al., *A novel hydrothermal synthesis of nanohydroxyapatite from eggshell-calcium-oxide precursors*, Heliyon 6 (2020) e03655.
45. D. Saha, L. Adak, M. Mukherjee and B. C. Ranu, *Hydroxyapatite-supported Cu(I)-catalysed cyanation of styrenyl bromides with K4[Fe(CN)6]: An easy access to cinnamonitriles*, Org. Biomol. Chem. 10 (2012) 952–957.
46. A. Noori, M. Hoseinpour, S. Kolivand, N. Lotfibakhshaiesh, S. Ebrahimi-Barough, J. Ai, and M. Azami, *Exploring the various effects of Cu doping in hydroxyapatite nanoparticle*, Sci. Rep. 14 (2024) 3724.
47. Y. Zhang, C. Lin, Q. Lin, Y. Jin, Y. Wang, Z. Zhang, et al., *CuI-BiOI/Cu film for enhanced photo-induced charge separation and visible-light antibacterial activity*, Appl. Catal. B. 235 (2018) 238–245.
48. Y. Wang, R. Wang, Y. Hu, L. Zheng, G. Fu, G. Wang, et al., *Impact of nanoscale Cu(I) precursors prepared by solution process on large-area CdTe solar cells*, Mater. Sci. Semicond. Process 181 (2024) 108652.
49. B. Putrakumar, P. K. Seelam, G. Srinivasarao, K. Rajan, R. Rajesh, K. R. Rao, et al., *High performance and sustainable copper-modified hydroxyapatite catalysts for catalytic transfer hydrogenation of furfural*, Catalysts 10 (2020) 1045.
50. G. Lin, F. Zhao, Y. Zhao, D. Zhang, L. Yang, X. Xue, et al., *Luminescence properties and mechanisms of CuI thin films fabricated by vapor iodization of copper films*, Materials 9 (2016) 990.
51. C. S. Ciobanu, D. Predoi, S. L. Iconaru, M. V. Predoi, L. Ghegoiu, N.

Buton, et al., *Copper doped hydroxyapatite nanocomposite thin films: synthesis, physico–chemical and biological evaluation*, BioMetals 37 (2024) 1487–1500.

52. A. S. Khan and M. Awais, *Low-cost deposition of antibacterial ion-substituted hydroxyapatite coatings onto 316L stainless steel for biomedical and dental applications*, Coatings. 10 (2020) 880.
53. N. Méndez-Lozano, M. Apatiga-Castro, A. de J. Ruíz-Baltazar, M. de la Luz-Asunción and E. E. Pérez-Ramírez, *Characterization and Evaluation of Silver Concentrations in Hydroxyapatite Powders*, J. Funct. Biomater. 14 (2023) 467.
54. R. Rosley, N. A. Badarulzaman, S. S. Suradi and H. Dzinun, *Preparation and Characterization of Hydroxyapatite Using Precursor Extracted from Cockle Shell Waste*, Paper Asia 40 (2024) 248–253.
55. I. Wahda, S. Kasim, M. Maming, H. Natsir, S. Fauziah, Y. Hala, et al., *Synthesis and characterization of hydroxyapatite/SiO_2/gelatin composites as bone scaffold candidates*, Communications in Science and Technology 9 (2024) 16–24.
56. Yudha P. Budiman, Stephen A. Westcott, Udo Radius, Todd B. Marder, *Fluorinated Aryl Boronates as Building Blocks in Organic Synthesis,* Advanced Synthesis & Catalysis 363 (2020) 2224-2255.
57. D. Kiani and J. Baltrusaitis, *Surface chemistry of hydroxyapatite for sustainable n-butanol production from bio-ethanol*, Chem Catal. 1 (2021) 782–801.
58. V. Bilakanti, V. Boosa, V. K. Velisoju, N. Gutta, S. Medak and V. Akula, *Role of Surface Basic Sites in Sonogashira Coupling Reaction over Ca5(PO4)3OH Supported Pd Catalyst*, J. Phys. Chem. C. 121 (2017) 22191–22198.
59. M. G. Galloni, S. Campisi, A. Gervasini, S. Morandi and M. Manzoli, *How hydroxyapatite governs surface Cu(II) and Fe(III) structuring: Effects in the N2O decomposition under highly oxidant atmosphere*, Appl. Catal. A Gen. 655 (2023) 119101.
60. H. Brasil, A. F. B. Bittencourt, K. C. E. S. Yokoo, P. C. D. Mendes, L. G. Verga, K. F. Andriani, et al., *Synthesis modification of hydroxyapatite surface for ethanol conversion: The role of the acidic/basic sites ratio*, J. Catal. 404 (2021) 802–813.
61. C. H. Bartholomew, *Mechanisms of catalyst deactivation*, Appl. Catal. A Gen. 212 (2001) 17–60.
62. D. L. Trimm, *The regeneration or disposal of deactivated heterogeneous catalysts*, Appl. Catal. A Gen. 212 (2001) 153–160.
63. P. M. Álvarez, D. McLurgh and P. Plucinski, *Copper oxide mounted on activated carbon as catalyst for wet air oxidation of aqueous phenol. 2. Catalyst stability*, Ind. Eng. Chem. Res. 41 (2002) 2153–2158.
64. A. Amedlous, O. Amadine, Y. Essamlali, H. Maati, N. Semlal and M. Zahouily, *Copper Loaded Hydroxyapatite Nanoparticles as eco-friendly Fenton-like catalyst to Effectively Remove Organic Dyes*, J. Environ. Chem. Eng. 9 (2021) 105501.
65. H. Tounsi, S. Djemal, C. Petitto and G. Delahay, *Copper loaded hydroxyapatite catalyst for selective catalytic reduction of nitric oxide with ammonia*, Appl. Catal. B 107 (2011) 158–163.
66. P. Puthiaraj, P. Suresh and K. Pitchumani, *Aerobic homocoupling of arylboronic acids catalysed by copper terephthalate metal–organic frameworks*, Green Chem. 16 (2014) 2865–2875.
67. A. R. Liandi, A. A. Al-wahid, Y. D. I. Siregar, T. P. Wendari, A. H. Cahyana and A. Insani, *Green mussel shell-derived hydroxyapatite-CoFe2O4 catalyst: Microwave-assisted synthesis of 2-amino-4H-chromene derivative*, Case Stud. Chem. Environ. Eng. 10 (2024) 100851.
68. Yudha P. Budiman, Muhamad R. S. Sidik, Muhamad Diki Permana, Kansy Haikal, Iis I. Widiyowati, Yessi Permana, et al, *Catalytic efficiency of Cu-MOFs: HKUST-1 and CuBDC for the protodeboronation of aryl boronic acids*, RSC Adv. 15 (2025) 29453-29461
69. L. Sarah, J. Skraba, H. Carter J., and J. Richard P., *Acid-catalyzed rearrangements in arenes: interconversions in the quaterphenyl series*, Beilstein J. Org. Chem. 15 (2019) 2655–2663.
70. SpectraBase. *^{1}H NMR Spectrum of 1,4-Diphenyl-1,3-butadiene*; SpectraBase: Wilmington, DE, USA.